

Stephan A. Bolliger,¹ M.D.; Lars Oesterhelweg,¹ M.D.; Danny Spendlove,¹ M.D.; Steffen Ross,¹ M.D.; and Michael J. Thali,¹ M.D.

Is Differentiation of Frequently Encountered Foreign Bodies in Corpses Possible by Hounsfield Density Measurement?

ABSTRACT: The radiological determination of foreign objects in corpses can be difficult if they are fragmented or deformed. With multislice computed tomography, radiodensities—referred to as Hounsfield units (HU)—can be measured. We examined the possibility of differentiating 21 frequently occurring foreign bodies, such as metals, rocks, and different manmade materials by virtue of their HU values. Gold, steel, and brass showed mean HU values of 30671–30710 (upper measurable limit), mean HU values for steel, silver, copper, and limestone were 20346, 16949, 14033, and 2765, respectively. The group consisting of objects, such as aluminum, tarmac, car front-window glass, and other rocks, displayed mean HU values of 2329–2131 HU. The mean HU value of bottle glass and car side-window glass was 2088, whereas windowpane glass was 493. HU value determination may therefore help in preautopsy differentiation between case-relevant and irrelevant foreign bodies and thus be useful for autopsy planning and extraction of the objects in question.

KEYWORDS: forensic science, forensic imaging, Virtopsy, multislice computed tomography, foreign body detection, Hounsfield units

The detection and examination of foreign bodies within a corpse is enormously important in forensic pathology. In gunshot cases, for example, the foreign body may be a projectile, which may not only lead to the identification of the ammunition used, but often even the individual weapon (1). Furthermore, fragments of intermediate targets such as a window pane may be found in the corpse, thus permitting a reconstruction of the shooting and perhaps even the crime scene.

Traditionally, foreign bodies have been sought for using X-rays (2). X-ray machines allow for the detection of even very small objects with great precision and facilitate their extraction and subsequent examination at autopsy. Since the first forensic computed tomography in 1977 (3), several groups have implemented multislice computed tomography (MSCT) for the examination of corpses with considerable success (4–7), and also regarding foreign body detection (8–10).

However, in the autopsy of severely injured victims of traffic accidents or explosions, a large variety of deformed foreign bodies may be encountered. Obviously, not all of these objects warrant further examination after extraction. It may therefore be useful to know prior to autopsy where objects of interest such as bomb components are located, and where the forensically less important—albeit occasionally lethal—debris such as concrete fragments is located. However, as the original structure of these deformed objects or fragments may vary considerably from the original form, the determination of their nature can prove impossible with radiological methods.

MSCT has—apart from the possibility to locate and depict such objects in a three-dimensional fashion rapidly—a great advantage compared with X-ray; it allows discrimination between different

radiodensities. These radiodensities are graded in “Hounsfield Units” (HU) which represent the X-ray attenuation of materials in CT scan interpretation. Objects with a high density and atomic number will have a high HU and vice versa. These HU therefore represent radiological material constants. For example, air (at standard temperature and pressure) has a value of –1000 HU; water, 0 HU; fat between –50 and –100 HU; and bone 500 to 1000 HU.

The clinical observation of HU representing material constants has also been applied to foreign objects such as dental fillings (11,12), swallowed opium packets (13), and wood (14–16). Indeed, wood can mimic air (14,17) but tends to increase in attenuation after absorbing blood and blood products (16). Different types of wood have different attenuations (17).

However, we found no information on the HU values of other frequently encountered foreign bodies in forensic practice, such as metals, glass, rocks, and building material. We measured the HU of objects frequently found in corpses in Central/Western Europe and tried to differentiate them based on the respective HU values. Although plastics are also regularly found foreign bodies in corpses, we refrained from including these materials in our study due to the vast range of possible materials and enormously diverse consistency. A feature not examined in this study was the physical density, as the aim of this study was to differentiate foreign bodies solely by virtue of their radiological, and not their physical or chemical properties.

Methods and Materials

Scanning

The materials to be measured were placed on a polystyrene board on the CT table. MSCT scanning was performed on a Somatom Emotion 6 Scanner (Siemens Medical Solutions, Forchheim, Germany) with 6 × 1 mm collimation at 130 kV and 160 mAs.

¹Centre for Forensic Imaging and Virtopsy, Institute of Forensic Medicine, University of Bern, Bern CH-3012, Switzerland.

Received 28 Jan. 2008; and in revised form 2 Oct. 2008; accepted 3 Oct. 2008.

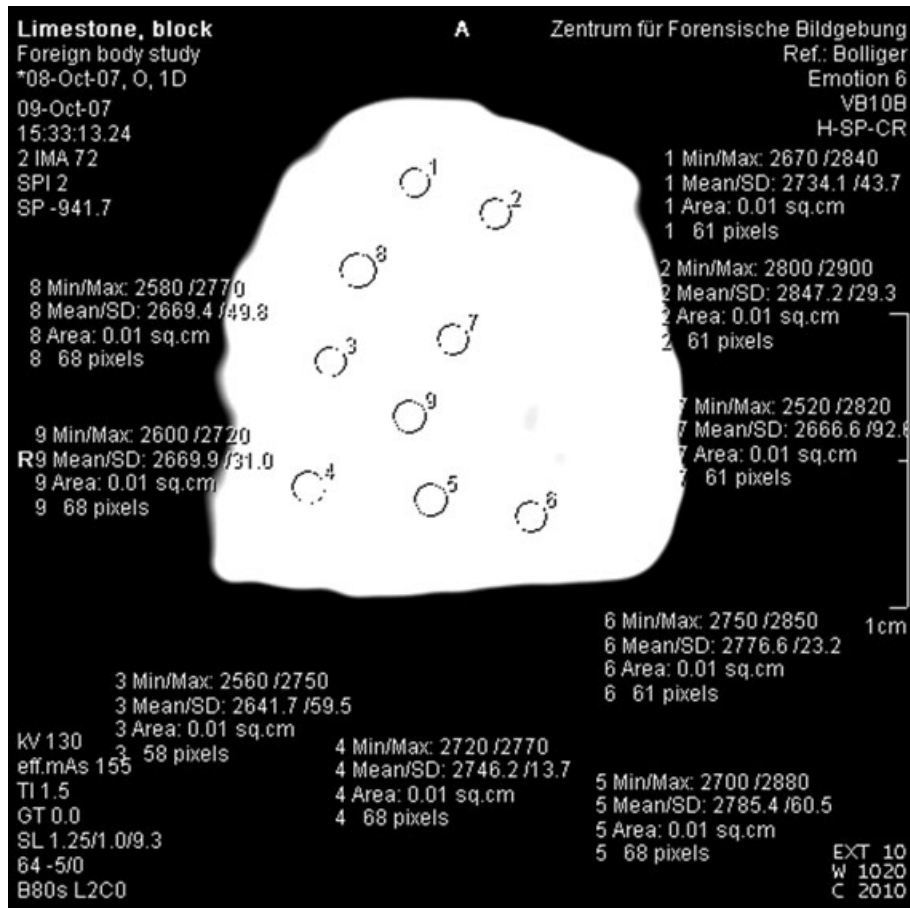


FIG. 1—Exemplary measurement of a limestone block. A circle of 0.01 cm^2 is placed well away from the surface in order to prevent beam-hardening artifacts. On this image, no measurements were made. The software automatically calculates the minimum, maximum, and mean Hounsfield units as well as the SD.

TABLE 1—The examined materials are listed according to decreasing mean Hounsfield units (HU) values.

Material	Mean HU	SD	Minimum HU	Maximum HU
Gold	30710*	0	30710*	30710*
Lead	30674	83.11	30305	30710*
Brass	30671	145.3	26960	30710*
Steel	20346	63.6	19720	22490
Silver	16949	247.7	15560	22550
Copper	14033	536.8	11080	16980
Limestone	2765	41.4	2520	2940
Aluminum	2329	023.8	2230	2480
Marble	2289	81.6	1810	2780
Tarmac	2251	108.7	1520	2990
Car glass front	2260	105.3	1640	2830
Slate	2208	33.4	1820	2670
Granite	2131	109.8	1730	2830
Bottle	2088	41.23	1996	2408
Car glass side	2088	57.8	1970	2760
Quartzite	1751	39.8	1420	1930
Sandstone	1625	41.5	1400	1910
Tile	1548	15.0	1440	1740
Cement	1423	81.6	750	1960
Pottery	1417	17.5	1240	1580
Window pane	493	56.8	330	810

The SD as well as the minimum and maximum Hounsfield unit values are given. The limit of our scanner was 30710 HU.

*Indicates the maximum measured value. In effect, the material could present a far higher HU value.

Image reconstruction was carried out in 1.25-mm-slice thickness (0.7 mm reconstruction interval), extended CT scale and a hard kernel (B80s).

With this extended CT scale, a maximum of 30710 HU could be detected. On the hereby obtained images, a 0.01 cm^2 region was encircled and the mean, maximum, and minimum HU values were measured by the software (Leonardo, Siemens Medical Solutions) and the SD automatically calculated. Due to beam hardening artifacts, great care was taken to avoid the surface-near portions (Fig. 1). Thirty measurements were performed on each of these 21 material samples of varying sizes.

Metals

We studied seven metals, namely, gold (20 Swiss franc gold coin, a "Vreneli," and 900 fine gold), silver (a bar of pure [$>99\%$] silver), brass (nails), lead (pure lead shotgun pellets), copper (pure copper wire), steel (steel screws), and aluminum (part of a pure aluminum window frame).

Stones

Six types of rock frequently found in Western and Central Europe and occasionally used in the construction of buildings and roads (kerbstones and cobblestones) were examined, including granite, quartzite, marble, limestone, slate, and sandstone.

Man-made Materials

We examined four types of glass, namely, bottle glass, glass from a window pane, wind-shield glass, and side-window glass from motor cars. Two types of baked clay were included: bathroom tile and a red clay flowerpot. We also scanned housing cement and tarmac.

Results

The measured HU of the materials are listed in Table 1. Figure 2 gives an overview of the results. Not surprisingly, the metals (with the exception of aluminum) displayed the highest HU densities. Gold, lead, and brass showed mean HU values of 30671–30710, which were at the top end of the measurable scale of our CT (30710 HU) unit and could in reality be much higher. Due to the overlapping SD ranges (mean value ± SD), these objects could be distinguished from each other by their radiodensities.

Steel, silver, and copper displayed different radiodensities of 20346, 16949, and 14033 HU respectively. As the SD ranges of these three metals did not overlap, they were readily discernible from each other. Limestone proved to be rather radioopaque compared with the other nonmetallic materials (see Fig. 3) with a mean HU value of 2765 (SD: 41 HU).

Aluminum, marble, tarmac, car window glass (front and side windows), slate, granite, and bottle glass displayed HU values of 2329–2088. The SD ranges and minimum and maximum values of these materials are shown in Fig. 4. Aluminum, marble, tarmac,

and car front-window had overlapping SD ranges. Marble, tarmac, car front-window, slate, and granite showed overlapping values, whereas granite, bottle glass, and car side-window glass displayed overlapping SD ranges. Therefore, aluminum could be distinguished from granite but the latter not from bottle glass, etc. Quartzite, sandstone, and tile ranged between 1548 and 1751 HU. Cement and pottery were found in the range of 1000–1500 HU and the glass of a window pane displayed a mean radiodensity of 493 HU (SD 56 HU).

Discussion

By measuring the HU opacity of a foreign object, it is possible to draw certain cautious conclusions as to the type of material involved. For example, if the object displays HU values of around 30710, it is most likely that it is gold, lead, or brass. Obviously other, rare materials with a high physical density, such as tungsten, or radioactive materials, such as uranium, plutonium, etc. cannot be excluded. These materials could be clearly differentiated from steel which has a mean HU value of 20346. Therefore in the case of a gunshot, the determination of whether a radioopaque fragment within the body belongs to the forensically less relevant lead core or to the steel jacket with its important rifling characteristics can easily be made. In cases of bomb explosions, metallic parts of the bomb can be distinguished from secondary fragments such as building material prior to autopsy, thus facilitating autopsy planning.

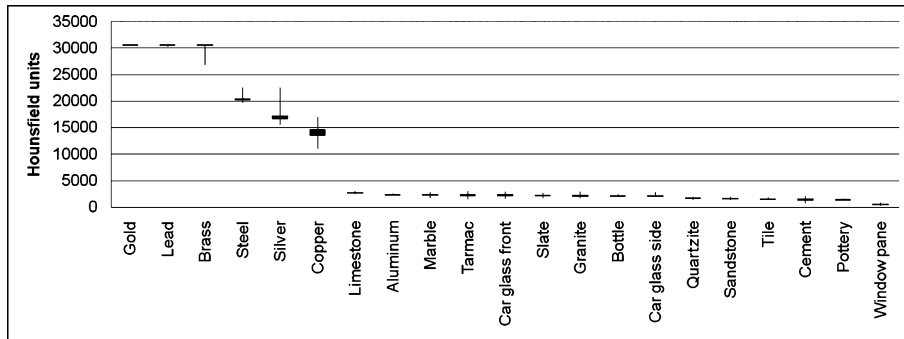


FIG. 2—Box-plot showing the upper and lower quartiles of the materials as a box with the maximum and minimum measurements as lines protruding from these.

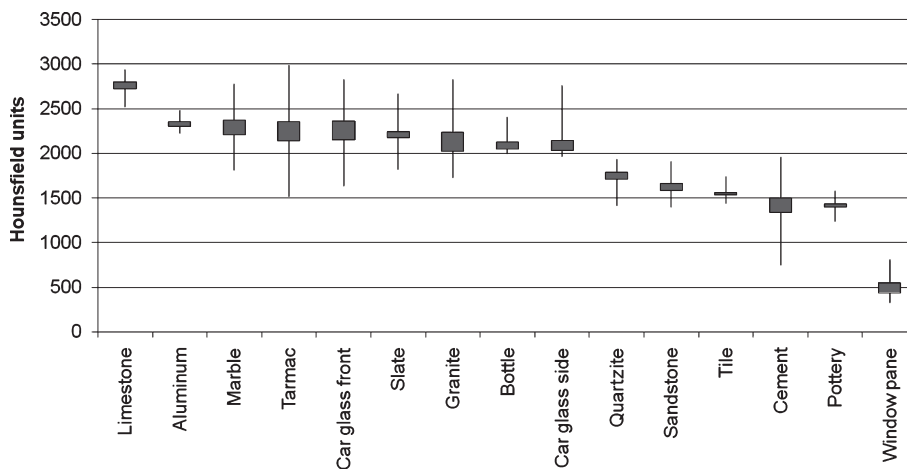


FIG. 3—Details of Fig. 2.

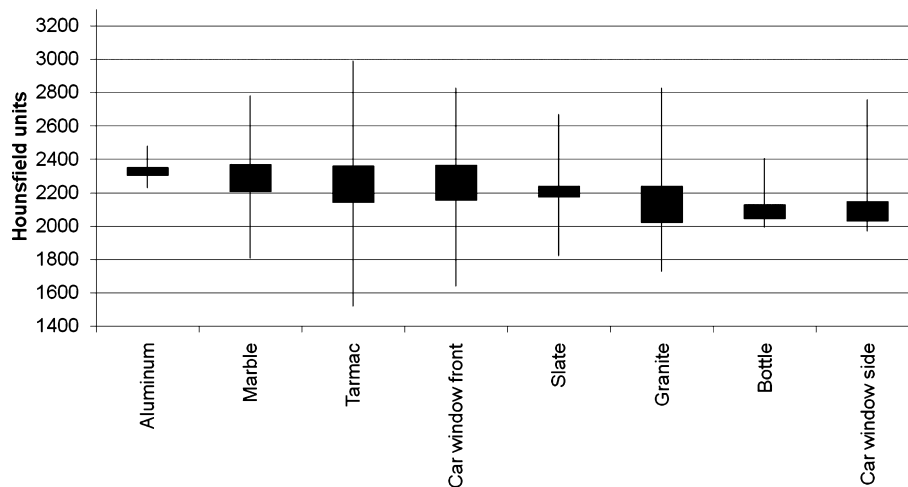


FIG. 4—Details of Fig. 3.

However, certain difficulties may arise regarding the size of the object in order to counter the beam hardening effect of the interface of the object with the surrounding tissue; the object's center must be measured keeping well clear of the surface-near regions. In very small objects, this may not be possible, thus rendering the measurement less reliable.

Another problem is the purity of the object. We only studied objects with a high grade of purity; for example, the gold of the "Vreneli" coin was 900 fine. Other, lesser gold alloys may show different HU values. Mixing of, for example, molten tarmac with other materials may also alter the mean HU density.

This study only examined a small portion of possible foreign objects within a human body. In order to create a systematic database of the HU values of foreign bodies, a vast number of such objects should be studied.

Conclusions

By measuring the HU values of foreign bodies, a certain triage between forensically relevant and less relevant objects can be made. This can facilitate autopsy planning and the extraction of the bodies in question. For this, a database with the HU values of a large amount of materials is necessary.

Acknowledgment

We would like to thank Werner Bolliger, PhD, for assistance in manuscript preparation and advice concerning European geology.

References

- Di Maio VJM, editor. Gunshot wounds: practical aspects of firearms, ballistics, and forensic techniques. Boca Raton: CRC Press, 1996.
- Brogdon BG, editor. Forensic radiology. 1st ed. Boca Raton, FL: CRC Press, 1998.
- Wullenweber R, Schneider V, Grumme T. Computertomographische Untersuchungen bei Schädel-Schuss-Verletzungen Z Rechtsmed. Z Rechtsmed 1977;80(3):227–46.
- Donchin Y, Rivkind AI, Bar-Ziv J, Hiss J, Almog J, Drescher M. Utility of post-mortem computed tomography in trauma victims. J Trauma 1994;37(4):552–5.
- Thali MJ, Yen K, Schweitzer W, Vock P, Boesch C, Ozdoba C, et al. Virtopsy, a new imaging horizon in forensic pathology: virtual autopsy by postmortem multislice computed tomography (MSCT) and magnetic resonance imaging (MRI)—a feasibility study. J Forensic Sci 2003; 48(2):386–403.
- Poulsen K, Simonsen J. Computed tomography in connection with medico-legal autopsies. Forensic Sci Int 2007;171 (2-3):190–7.
- Ljung P, Winskog C, Persson A, Lundstrom C, Ynnerman A. Full body virtual autopsies using a state-of-the-art volume rendering pipeline. Trans Vis Comput Graph 2006;12(5):869–76.
- Thali MJ, Yen K, Vock P, Ozdoba C, Kneubuehl B, Sonnenschein M, et al. Image-guided virtual autopsy findings of gunshot victims performed with multi-slice computed tomography (MSCT) and magnetic resonance imaging (MRI), and subsequent correlation between radiology and autopsy findings. Forensic Sci Int 2003;138 (1-3):8–16.
- Harcke HT, Levy AD, Abbott RM, Mallak CT, Getz JM, Champion HR, et al. Autopsy radiography. Digital radiographs (DR) vs multidetector computed tomography (MDCT) in high velocity gunshot-wound victims. Am J Forensic Med Pathol 2007;28(1):13–9.
- Thali MJ, Schwab CM, Tairi K, Dirnhofer R, Vock P. Forensic radiology with cross-section modalities: spiral CT evaluation of a knife wound to the aorta. J Forensic Sci 2002;47(5):1041–5.
- Jackowski C, Lussi A, Classens M, Kilchoer T, Bolliger S, Aghayev E, et al. Extended CT scale overcomes restoration caused streak artifacts for dental identification in CT-3D color encoded automatic discrimination of dental restorations. J Comput Assist Tomogr 2006;30(3):510–3.
- Jackowski C, Wyss M, Persson A, Classens M, Thali MJ, Lussi A. Ultra high resolution dual source CT for forensic dental visualization—discrimination of ceramic and composite fillings. Int J Legal Med 2008; 122(4):301–7.
- Taheri MS, Hassanian-Moghaddam H, Birang S, Hemadi H, Shahnazi M, Jalali AH, et al. Swallowed opium packets: CT diagnosis. Abdom Imaging 2008;33(3):262–6.
- Ho VT, McGuckin JF, Smergel EM. Intraorbital wooden foreign body: CT and MR appearance. AJNR Am J Neuroradiol 1996;17(1):134–6.
- Ginsberg LE, Williams DW, Mathew VP. CT in penetrating craniocervical injury by wooden foreign bodies: reminder of a pitfall. AJNR Am J Neuroradiol 1993;14(4):892–5.
- McGuckin JF, Akhtar N, Ho VT, Smergel EM, Kubacki EJ, Villafana T. CT and MR evaluation of a wooden foreign body in an in vitro model of the orbit. AJNR Am J Neuroradiol 1996;17(1):129–33.
- Roberts CF, Leehey PJ III. Intraorbital wood foreign body mimicking air at CT. Radiology 1992;185(2):507–8.

Additional information and reprint requests:
Stephan A. Bolliger, M.D.
Centre for Forensic Imaging and Virtopsy
Institute of Forensic Medicine
University of Bern
Buehlstrasse 20
CH 3012 Bern
Switzerland
E-mail: stephan.bolliger@irm.unibe.ch